Characterization and comparison of the intestinal microbiota in Chinese Shanxi black pig during the weaning and nursery periods

Pengfei Gao [1], **Haizhen Wang** [1], **Zhimin Cheng** [1], **Yuanyuan Wang** [1], **Pengkang Song** [1], **Xiaohong Guo** [1], **Zhibian Duan** [1], **Guoqing Cao** [1], **Jianfeng Liu** [2], **Min Du** [3], **Bugao Li** [Corresp. 1]

[1] Department of Animal Sciences and Veterinary Medicine, Shanxi Agricultural University, Taigu, China

[2] College of Animal Science and Technology, China Agricultural University, Beijing, China, China

[3] Department of Animal Sciences, Washington State University, Pullman, WA, USA

Corresponding Author: Bugao Li
Email address: bugaoli@yeah.net

Background. The intestinal microbiota plays essential functions that affect piglet health at the weaning stage. However, our understanding of the succession of bacterial intestinal communities during weaning and Nursery Periods of pig is limited.

Methods. To better understand this, we performed 16S rDNA gene sequencing of the contents of four distinct intestinal segments [duodenum (D), jejunum (J), ileum (I), and cecum (C)] in six Chinese Shanxi Black pigs at day 25 (B25 group; i.e., weaning) and day 70 (B70 group; i.e., nursery).

Results. We found that the dominant phyla are Proteobacteria, Bacteroidetes, and Firmicutes. In addition, the dominant genera were *Acinetobacter*, *Prevotella*, *Streptococcus*, and SMB53 (Clostridiaceae). The microbiota in the B25 group across segments were significantly different from that in the corresponding segments in the B70 group. In addition, the distinct segments in the B70 group presented a continuum consisting of compartmentalized architecture whereas the distinct segments in B25 group were relatively similar. The predicted molecular function analysis revealed higher enrichments in associated metabolisms as well as stress-induced functions in the B25 group.

Conclusions. This study provides insights into the succession of intestinal microbiota in Chinese Shanxi Black pigs before and after weaning, and provides reference for improving the intestinal development of piglets.

Characterization and comparison of the intestinal microbiota in Chinese Shanxi Black pig during the weaning and nursery periods

Pengfei Gao[1], Haizhen Wang[1], Zhimin Cheng[1], Yuanyuan Wang[1], Pengkang Song[1], Xiaohong Guo[1], Zhibian Duan[1], Guoqing Cao[1], Jianfeng Liu[2], Min Du[3], Bugao Li[1*]

1, Department of Animal Sciences and Veterinary Medicine, Shanxi Agricultural University, Taigu, Shanxi, China

2, College of Animal Science and Technology, China Agricultural University, Beijing, China

3, Department of Animal Sciences, Washington State University, Pullman, WA, USA

[*]**Corresponding author: Bugao Li,** Email: bugaoli@yeah.net

ABSTRACT:

Background. The intestinal microbiota plays essential functions that affect piglet health at the weaning stage. However, our understanding of the succession of bacterial intestinal communities during weaning and Nursery Periods of pig is limited.

Methods. To better understand this, we performed 16S rDNA gene sequencing of the contents of four distinct intestinal segments [duodenum (D), jejunum (J), ileum (I), and cecum (C)] in six Chinese Shanxi Black pigs at day 25 (B25 group; i.e., weaning) and day 70 (B70 group; i.e., nursery).

Results. We found that the dominant phyla are Proteobacteria, Bacteroidetes, and Firmicutes. In addition, the dominant genera were *Acinetobacter*, *Prevotella*, *Streptococcus*, and SMB53 (Clostridiaceae). The microbiota in the B25 group across segments were significantly different from that in the corresponding segments in the B70 group. In addition, the distinct segments in the B70 group presented a continuum consisting of compartmentalized architecture whereas the distinct segments in B25 group were relatively similar. The predicted molecular function analysis revealed higher enrichments in associated metabolisms as well as stress-induced functions in the B25 group.

Conclusions. This study provides insights into the succession of intestinal microbiota in Chinese Shanxi Black pigs before and after weaning, and provides reference for improving the intestinal development of piglets.

Key words: Gut microbiota; Functional capacity; 16S rRNA; Weaning and nursery periods; Chinese Shanxi Black pigs

INTRODUCTION

Intestinal microbiota play essential roles in the maintenance of growth and health of hosts (Hillman et al. 2017; Sommer & Backhed 2013). Recent studies reported that perturbation of the microbial communities in mammalian intestinal tract is closely related to metabolic diseases, chronic inflammation, and cancer (Kashyap et al. 2017; Tian et al. 2017). During the weaning stage, a piglet is challenged by drastic alterations in bacterial exposure and dietary nutrition (Liu et al. 2018). Therefore, the process of bacterial community succession is vulnerable to multiple factors, such as dietary contamination, environmental exposure, and physiological loss of hemostasis. Disturbed transitions might render the piglet more susceptible to infection and nutritional disorders, which would interfere with its growth and development. Thus, the weaning stage was regarded as a necessary period for introducing antibiotics into the dietaries. However, several scientists are concerned that the abuse of antibiotics in livestock industry might cause damage of consumers' health and give rise to excessive bacterial resistance, thereby endangering both animals and humans (Costa et al. 2015). There has been a general trend among food administrations to ban or limit the use of antibiotics in livestock business. Although using antibiotics have reduced the total infections, the diversity of colonized bacteria is could be underestimated, which might explain the occurrences of diarrhea in some weaned piglets fed with antibiotics. Thus, substitutes for antibiotics, which can prevent infections at the weaning stage, are urgently required. Evidence suggesting that probiotics, as alternatives to antibiotics, have positive effects in controlling infection and promoting growth mainly due to the competitive exclusion of pathogenic bacteria, has emerged (Inatomi et al. 2017; Kim et al. 2018).

However, deciding which kind of prebiotics might have positive effects on piglets is difficult to predict. Screening effective prebiotics candidates can be time-consuming and labor intensive. Detecting prebiotics from pigs and turning it into food additive for the same species might be a solution to the problem. Therefore, this study applied 16S rDNA gene sequencing (Cole et al. 2014) to characterize and compare the compositions and phylogenetic distributions of the microbiota within the distinct intestinal compartments [duodenum (D), jejunum (J), ileum (I), and cecum (C)] of Chinese Shanxi Black piglets at lactation and post-weaning stages, and applied an inferred pathway analysis to investigate the functional differences of the communities. The major aim was to understand the phylogenic constructions of their intestinal microbiota and providing guidance for the screening of candidate prebiotics for piglets in the transition period of weaning.

MATERIALS & METHODS

Animals

All experimental procedures on animals were conducted in accordance with the Code of Ethics of the World Medical Association (Declaration of Helsinki) for animal experiments (http://ec.europa.eu/environment/chemicals/lab_animals/legislation_en.htm). The methods were performed in accordance with the Good Experimental Practices adopted by the College of Animal Science and Veterinary Medicine, Shanxi Agricultural University and the experimental protocols were approved by it.

Six Shanxi Black pigs were used in this study. The individuals were raised at the Datong Pig Breeding Farm (Shanxi, China) with standard dietaries (Council 2012). Piglets were weaned 24 d

after birth. Three piglets were sacrificed at the age of 25 d (B25 group), and the other three were sacrificed at the age of 70 d (B70 group). The pigs were fasted for 12 h with free access to fresh water, and then sacrificed at the Datong slaughtering management office designated for pigs according to standard procedures. The pigs were dissected for sample collection from the intestinal tracts of D, J, I, and C. The samples were indexed as a letter standing for the segment and an Arabic numeral for pig recognition. For instance, B25 I1 means sample ileum of pig 1 in the group of piglets at the age of 25 d.

Total bacterial genomic DNA extraction and 16S rDNA sequencing

For 16S rRNA gene sequencing, the total genomic DNA of each sample was extracted using the QIAamp Fast DNA Stool Mini Kit (Qiagen, Valencia, CA, USA) according to manufacturer's instructions (Mao et al. 2012). Thereafter, the V3 to V4 hypervariable regions of 16S rRNA gene were amplified using polymerase chain reaction (PCR) in 25 mL reactions containing 0.2 mM each primer (341F: 5′-CCTAYGGGRBGCASCAG-3′; 806R: 5′-GGACTACNNGGGTATCTAAT-3′), 50 ng DNA template, and 12.5 μL PCR premix (16S rDNA Bacterial Identification PCR Kit, TaKaRa, Dalian, China). The applied reaction conditions were as follows: 94 °C (4 min), followed by 25 cycles of 94 °C (30 s), 55 °C (30 s), and 72 °C (30 s), with a final extension at 72 °C (10 min) (Costa et al. 2012). The PCR products were purified from agarose gels with DNA gel extraction kit (Tiangen, Beijing, China). The DNA amplicon concentration of each group was assessed with Quant iFluor^{TM} (Promega, Madison, WI, USA) for subsequent sequencing library construction with Celemics (Celemics, Inc., Seoul, Korea). The barcoded libraries were detected with paired-end 250 bp sequence reads from an Illumina Hiseq

2500 platform (Illumina, San Diego, CA, USA) (Caporaso et al. 2012).

Tag and operational taxonomic unit (OTU) assessment

From the raw FASTQ files of the reads obtained, we trimmed the primer and adapter sequences. Thereafter, sequences containing more than 10% of the unknown nucleotides (N) or 20% of low quality (Q-value <20) bases were eliminated. Sequences mapped to chloroplast or mitochondria genome were discarded. Moreover, tags were generated according to alignment between paired-end reads, which shared more than 10 bp overlap, and less than 2% mismatch. Subsequently, we removed the redundant tags to generate the unique-tag datasets (Campbell et al. 2010). DNA distance matrices were clustered to count OTUs at 3.0% sequence divergences in the communities. Community diversity was assessed using the combination of bias-corrected Chao1 richness estimator, the abundance of coverage estimator (ACE), the diversity indices of Shannon, npShannon, and Simpson, and the coverage percentage. All analyses mentioned above were conducted using the software of MOTHUR (Schloss et al. 2009). Differentiation diversities were evaluated by the indices of beta diversities, which were calculated by dividing the common OTUs between two samples to the ratio of all OTUs (Kemp & Aller 2004).

Taxonomic abundance profiling

A naive Bayesian-based classifier (rdp) was used to classify taxonomy of the tags by comparing them with the Greengenes database (version 20101006) (DeSantis et al. 2006). The confidence threshold was 0.5. The OTUs were categorized based on the tag annotation. The procedures complied with the mode principle, where more than 66% of the tags were demanded to rationalize the same level in the series of domain, phylum, class, order, family, genus, and

119 species.

120 For differentially abundant taxon identification in multiple segments within one group of pigs,
121 we applied linear discriminant analysis (LDA) effect size (LEfSe) method (Segata et al. 2011).
122 Briefly, the Kruskal-Wallis rank sum test was run to detect features with significantly different
123 abundances among all groups. Thereafter, Wilcoxon rank sum test was used to detect features,
124 after which LDA estimation was performed. In addition, a taxonomic cladogram representative of
125 the structure of microbial community of each sample and their predominant bacteria was drawn to
126 display the greatest differences in taxa among the samples. For identifying differentially abundant
127 taxa in the same segment between the different groups of pigs, the software Metastat was used
128 (White et al. 2009).

129 **Molecular functional enrichment prediction**

130 The software Phylogenetic Investigation of Communities by Reconstruction of Unobserved
131 States (PICRUSt) (Langille et al. 2013) was used to predict functional enrichment of the
132 communities in based on the information available in the Kyoto Encyclopedia of Genes and
133 Genomes (KEGG) database (Du et al. 2014). Correlation coefficients of the pathway enrichment
134 in the samples within the same group were calculated using the method of Spearmen (Julia et al.
135 2007). The R suite package, edgeR (Robinson et al. 2010), was used to determine differentiated
136 pathways under the control of $\log_2$ fold change > 2 and FDR < 0.01. Volcano plots and heatmaps
137 for the differentiated pathways were generated.

138 **RESULTS**

139 **Tag and OUT-based analysis**

After removing low-quality reads and chimeras of the Illumina sequenced reads, we obtained 2, 036, 183 unique tags covering 925, 528, 252 bases, with an average of 39, 937 tags per sample. The detailed tag status for each sample was listed in Table 1. OTU profiling was determined with an average number of 84,841 in each sample. Correlation coefficients of the samples derived from the same age, i.e. the B2 and B70 group, were calculated by Spearman's correlation analysis (Fig.1A). Generally, at the same age, samples of the same intestinal segments from different pigs were highly correlated with each other.

Thereafter, we performed principal component analysis (PCA) based on the OTU profiling (Fig.1B). The majority of the B25 samples were tightly clustered, whereas the B70 samples were divergently scattered. Therefore, we supposed that the intestinal segments in the B25 group were relatively similar in terms of microbial community composition. As illustrated in Fig.1C, the C of the pigs of the B25 and B70 groups had a similar yet distinguishable distribution. However, the B25 samples were distinct from the B70 samples in various segments, in spite of the omission of a sample each from B70 D, B70 J, and B25 I.

To analyze the alpha diversities of the samples, we calculated several indices as mentioned in the methods (Table 2). Firstly, with the coverage of all samples being higher than 90%, we inferred that the sequencing depth attained was sufficient to evaluate the diversities of the samples, which was further confirmed by the presence of plateaus in the Shannon-Wiener curves (Fig.1C). Subsequently, we have compared the other indices between the B25 and B70 groups. We have combined the D, I, J segments and labeled it as small intestine (SI) to distinguish it from the C samples.

Microbiota profiles of the distinctive intestinal segments

The phylum composition of each sample is listed in Supplementary Table S1. As illustrated in the stack plot of phylum proportions (Fig.2A), the majority of the obtained OTUs belonged to Proteobacteria, Bacteroidetes, and Firmicutes, which accounted for 95.5% ± 4.9% of the samples, although the I of pig 1 and 3 in the B25 group and that of pig 1 and 2 in the B70 group appeared to have >1% of Bacteroidetes. Cyanobacteria ranked fourth among the dominant phyla in the total microbiota. It had the most abundant distribution in the J of pig 2 in the B25 group and that of pig 3 in the B70 group, constituting up 21.6% and 10.8%, respectively, in the microbial communities.

The genus classification is listed in Supplementary Table S2. The genus with either low total richness (out of top 50) or small standard deviation (out of top 50) merged and labeled as "Others" for dimension reduction to generate the genus stack plot (Fig.2B). The result showed that the most predominant genera among all the samples were *Acinetobacter*, and that. SMB53 (Clostridiaceae) was the fourth highly enriched genus, whose total amount was mainly contributed by the unexpectedly high proportions in the I of pig 1 and 3 in the B25 group (71.4% and 65.5%), and in the J of pig 1 and 3 in the B70 group (21.6% and 22.0%). Comparing to the small intestinal segments, the C segments in the B25 and B70 group presented consistently low proportions of *Acinetobacter* (<1.5%). The most dominant genus in the C of the pigs of B25 was *Prevotella*, which constituted 42.1%, 61.4%, and 44.0%, respectively, in the three replicates, whereas in the C of the pigs of B70, the dominant genus was *Faecalibacterium*, with the proportions being 71.6%, 47.7%, 33.2%.

Intragroup comparison of bacterial microbiota among different intestinal segments

Intragroup comparison analysis was performed to investigate the differences of microbiota in the distinctive segments respectively in the B25 and B70 groups. Firstly, alpha diversities of the samples were analyzed by calculating the mentioned indices. When comparing the alpha diversity indices between intragroup segments, we merged the D, J, and I segments to form the SI group standing for the small intestine and compared it with C from the large intestine. As shown in Fig.2C, the C segments exhibited significantly lower ($P < 0.01$) Simpson index and higher ($P < 0.01$) Chao1, ACE, and Shannon index than in their respective SI segment, in both the B25 and B70 groups. This result indicated that, regardless of the growth stage, the C had more diversity in the microbial communities than in the small intestines. Thereafter, LEfSe analysis was applied to identify differentiated taxa between the distinctive segments in both porcine groups. LEfSe analysis revealed 3, 26, 15, and 14 specifically enriched taxa in the C, D, I, and J segments, respectively, in the B25 group (Supplementary Table S3 and Fig.3), and 17, 46, 3, and 13 enriched taxa, respectively, in the B70 group (Supplementary Table S4 and Fig.3). The result suggested that the porcine C and D were gaining more characteristic community structures from the weaning stage to the nursery stage. The B25 D, B25 J, B25 I, and B25 C samples had high abundances of *Acinetobacter* and *Campylobacter*, *Actinobacillus*, *Actinobacillus*, and *Bacteroides*, respectively. These genera contained predominantly gram-negative pathogens, which may induce infection or result in systematic inflammation. The B70 C samples had high abundances of the species *Faecalibacterium prausnitzii*. In adult mammals, *Faecalibacterium prausnitzii* represents more than 5% of the intestinal bacteria, making it one of the most commonly distributed species of gut bacteria. In addition, it was reported to boost the immune system. The B70 D samples were rich

in *Prevotella* species. It was claimed to be abundant in the gut, consume carbohydrates, especially fibers. These results reflected the change of nutrition source from breast milk to manufactured dietaries.

For functional analysis, the correlation coefficients revealed in the prediction analysis presented a similar pattern comparing to the correlation coefficient matrices of the OTUs (Fig.4). Due to the low correlation in the I and J of B25, and I and J of B70, the datasets were not powerful enough for inferring statistical significance among D, I, and J within each group. Therefore, we combined the D, I, and J segment datasets to form a representative of the small intestine, and compared it with the corresponding C dataset. Consequently, 58 and 17 kinds of significantly differentiated molecular functions were found in the B25 and B70 groups, respectively. Among the differences in the B25 group, the entire were elevated in the small intestine (Fig.4A-C). In addition, the functions differ mainly in the glycol metabolism and lipid metabolism pathways. Notably, the elevation of the penicillin-binding protein 1B was the highest in the small intestine of the B25 group. This result indicates a possibility that breast-feeding may expose a piglet to antibiotics administered to the mother pig, and therefore affect the intestinal microbiota. In the B70 group, levels of 13 out of the 17 kinds of functional molecules were elevated in the small intestine, including those of various nutritional processing enzymes (Fig.4D-F). Three out of the five types of enriched molecules from C were associated with glycol metabolism. In addition, the regulation of sporulation process was indicated by the higher presence of the inhibitor of the pro-sigma K processing machinery.

Intergroup comparison of bacterial microbiota among different intestinal segments

Firstly, beta diversity matrices of the two groups are listed in Table 3, respectively. The beta diversities between the small intestinal segments in the B70 group were significantly higher than those in the B25 group ($P < 0.01$). In addition, the beta diversities between the C and small intestinal segments in the B70 group were significantly larger than those in the B25 group ($P < 0.01$). Therefore, it appeared that the pigs at nursery periods had the lowest differentiation among segments ($P < 0.01$). The result suggested that the B25 group might have richer intestinal diversities than the B70 group, and that the pigs at weaning could be vulnerable.

Subsequently, analysis using Metastat for differentiated taxon identification the fixed segments between the two groups (Supplementary Table S5-S8). To evaluate the differentiation of the communities among the intestinal segments, the beta diversity matrices of each group were calculated and listed in Table 3. As we were interested in the successive change in every segment of the intestines of pigs. The comparative values generated from the samples of the same pig were considered to reflect successive alterations in microbial community composition in the different intestinal segments. It was observed that the beta diversities generated by comparing the microbial communities in the small intestinal segments, were significantly higher in the B70 group than those in the B25 group ($P < 0.01$). In addition, the beta diversities of C and each small intestinal segment were higher in the B70 group than in the B25 group ($P < 0.01$). Therefore, it appeared that the pigs at the nursery stage had more divergent microbial community structure among intestinal segments than the 25-day-old piglets.

For comparing the differences functional enrichment of the intestinal segments between B25 and B70 groups, the I (Fig.5A) and C (Fig.5B) segments presented significantly differentiated

molecular enrichments (24 and 16), whereas D and J did not. Among the differences, the majority were elevated in the B25 group, with one exception in the comparison of C. The result was consistent with the fact that the B25 group possesses a more diversified microbiota than the B70 group. The breast milk might be more enriched and contain more diverse nutrients than do manufactured dietaries; therefore, both the I and C segments in B25 group showed more enrichments in a variety of metabolic enzymes. However, it was intriguing to spot that the C of B25 were more enriched in multiple antibiotic resistance proteins, heavy metal exporters, and outer membrane channel proteins Tolc. In addition, differentiated pathways were identified based on the differential taxonomic composition revealed by the analysis using Metastat (Fig.5C-F). As shown in the figure, the major enriched pathways were associated with metabolism, particularly for carbon metabolism, and pathways associated with the biosynthesis of amino acids and proteins. The result was consistent with the fact that their carbon and nitrogen sources were altered. Moreover, the enrichment of galactose metabolism was consistent with the inferences of the molecular function prediction, because piglets leave a limited surplus of galactose for cecum microbes before the weaning stage.

DISCCUSSION

The pork-producing industry is facing substantial challenges, including abuse of antibiotics, failure of infection control, and nutritional malfunction, particularly at weaning and nursery stages when the gut microbial communities of piglets are immature and vulnerable (Hedegaard et al. 2017). Accumulating evidences suggest that the intestinal microbiota in mammals affect a vast range of metabolic activities associated with bacterial growth and exert considerable effects on the

health of the host (Conte et al. 2006; Shen 2017; Turnbaugh et al. 2006). Therefore, we had assumed that gut microbiota analysis might improve our capabilities in dealing with these problems. Recently, studies focusing on livestock gut microbiota were published, most of which were undertaken at a fixed age of the experimental animals (Mao et al. 2015; Schoster et al. 2013). In the present study, taxonomic classification raveled that the dominant taxa at the phylum level are Proteobacteria, Bacteroidetes, and Firmicutes, and those at the genus level are *Acinetobacter*, *Prevotella*, *Streptococcus*, and SMB53, consistent with associated studies on livestock intestinal microbiota. Functional analysis showed results that were consistent with relevant studies on humans, and some other mammals with the convergent presence of carbohydrate metabolism, amino acid metabolism, DNA replication and repair, and membrane transportation. However, we were surprised to find that the piglets presented more molecular mechanisms to cope with antibiotics, heavy metals, and toxins before weaning. It is plausible yet disturbing to infer that the breast milk is the source of the stresses because the mother pig could have accumulated more of these components than the pigs that were just starting to eat manufactured dietaries. Comparisons between the B25 and B70 groups showed that piglets at day 25 had a more diversified intestinal microbiota in the D, J, I, and C than the corresponding segments in pigs that have been weaned more than a month earlier. On the contrary, the intersegmental similarities in B70 pigs were smaller to those in B25 pigs. We inferred that the breast milk might have provided a more favorable nutrition source to the microbial communities, thus allowing a more diversified ecosystem in each segment. However, the dietaries provided after weaning were harder to decompose. Therefore, the different intestinal segments of B70 were organized into more compartmentalized units to

287 understand a serial continuum of functions to decompose the nutritious compounds. In addition,
288 breast-feeding would also help to explain the inference of increased alpha-galactosidase in the C
289 of B70 group, because mammals depend heavily on lactose metabolism at the weaning stage,
290 which leaves a limited surplus for intestinal microbes. In the weaning transition, the diet of the
291 piglets was changed from highly digestible milk to a less digestible solid feed. We concluded that
292 besides the age factor, the stress of weaning and shift in food composition might contribute to the
293 significant change in microbiota profiles.

294 To fulfill the goal of providing insightful clues for probiotics screening, we suggest chosen
295 candidates in the globally distributed genus, as a prerequisite for a probiotic to enhance host growth
296 is the origin from the pig gut microbiota itself (Strube et al. 2015). The characteristic high
297 proportion of *Faecalibacterium* in the C of B70 might have played a key effect in balancing the
298 microbiota and favoring host performance. Therefore, we would recommend considering
299 *Faecalibacterium* as a candidate genus for probiotics screening.

300 **CONCLUSIONS**

301 In conclusion, this study is the first to describe a comparison between the microbial
302 communities between weaning and nursery piglets, to the best of our knowledge. We found that
303 microbes in the various intestinal segments of weaned pigs undertakes to build sophisticated
304 architecture, which might be effective in performing organized functions as a continuum, although
305 the microbial community of every segment was less diversified than that of the corresponding
306 segment in piglets before weaning. Therefore, we would suggest introducing various kinds of
307 cooperative probiotics that harbor in different intestinal segments and help the piglets to deal with

stresses at the weaning and nursery stage.

ACKNOWLEDGMENTS

We would like to thank Guangzhou Gene denovo Biotechnology Co., Ltd. for 16S rRNA gene sequence and data analysis. We would like to thank Editage [www.editage.cn] for English language editing. The authors wish to thank the anonymous reviewers for their valuable comments and suggestions, which were helpful in improving our manuscript.

ADDITIONAL INFORMATION AND DECLARATIONS

Funding

The project was funded by the Special Fund for Sanjin Scholar, the Fund for Shanxi 1331 Project, Foundation of Science and Technology Achievements Transformation Projects in Shanxi Province (SXNKTG201701), and Postdoctoral fund of Shanxi Agricultural University.

Competing interests

The authors declare that they have no competing financial interests.

Authors' contributions

Pengfei Gao analyzed the data and drafted the manuscript under the supervision of Min Du and Bugao Li. Haizhen Wang, Zhimin Cheng and Pengkang Song carried out the bioinformatics analyses, under the supervision of Guoqing Cao and Jianfeng Liu. Zhibian Duan and Bugao Li conceived the study. Yuanyuan Wang prepared the samples, under the supervison of Xiaohong Guo and Pengfei Gao. All authors read and approved the final manuscript.

Data availability

The sequencing data from this study were deposited in the NCBI GEO database with the accession

number SRP115844.

REFERENCE

Campbell BJ, Polson SW, Hanson TE, Mack MC, and Schuur EA. 2010. The effect of nutrient deposition on bacterial communities in Arctic tundra soil. *Environmental Microbiology* 12:1842-1854. 10.1111/j.1462-2920.2010.02189.x

Caporaso JG, Lauber CL, Walters WA, Berg-Lyons D, Huntley J, Fierer N, Owens SM, Betley J, Fraser L, Bauer M, Gormley N, Gilbert JA, Smith G, and Knight R. 2012. Ultra-high-throughput microbial community analysis on the Illumina HiSeq and MiSeq platforms. *ISME J* 6:1621-1624. 10.1038/ismej.2012.8

Cole JR, Wang Q, Fish JA, Chai B, McGarrell DM, Sun Y, Brown CT, Porras-Alfaro A, Kuske CR, and Tiedje JM. 2014. Ribosomal Database Project: data and tools for high throughput rRNA analysis. *Nucleic Acids Research* 42:D633-642. 10.1093/nar/gkt1244

Conte MP, Schippa S, Zamboni I, Penta M, Chiarini F, Seganti L, Osborn J, Falconieri P, Borrelli O, and Cucchiara S. 2006. Gut-associated bacterial microbiota in paediatric patients with inflammatory bowel disease. *Gut* 55:1760-1767. 10.1136/gut.2005.078824

Costa MC, Arroyo LG, Allen-Vercoe E, Stampfli HR, Kim PT, Sturgeon A, and Weese JS. 2012. Comparison of the fecal microbiota of healthy horses and horses with colitis by high throughput sequencing of the V3-V5 region of the 16S rRNA gene. *PloS One* 7:e41484. 10.1371/journal.pone.0041484

Costa MC, Stämpfli HR, Arroyo LG, Allen-Vercoe E, Gomes RG, and Weese JS. 2015. Changes in the equine fecal microbiota associated with the use of systemic antimicrobial drugs. *BMC Veterinary Research* 11:19. 10.1186/s12917-015-0335-7

Council NR. 2012. *Nutrient Requirements of Swine: Eleventh Revised Edition*. Washington, DC: The National Academies Press.

DeSantis TZ, Hugenholtz P, Larsen N, Rojas M, Brodie EL, Keller K, Huber T, Dalevi D, Hu P, and Andersen GL. 2006. Greengenes, a chimera-checked 16S rRNA gene database and workbench compatible with ARB. *Applied and Environmental Microbiology* 72:5069-5072. 10.1128/AEM.03006-05

Du J, Yuan Z, Ma Z, Song J, Xie X, and Chen Y. 2014. KEGG-PATH: Kyoto encyclopedia of genes and genomes-based pathway analysis using a path analysis model. *Mol Biosyst* 10:2441-2447. 10.1039/c4mb00287c

Hedegaard CJ, Lauridsen C, and Heegaard PMH. 2017. Purified natural pig immunoglobulins can substitute dietary zinc in reducing piglet post weaning diarrhoea. *Veterinary Immunology and Immunopathology* 186:9-14. https://doi.org/10.1016/j.vetimm.2017.02.001

Hillman ET, Lu H, Yao T, and Nakatsu CH. 2017. Microbial Ecology along the Gastrointestinal Tract. *Microbes and Environments* 32:300-313. 10.1264/jsme2.ME17017

Inatomi T, Amatatsu M, Romero-Perez GA, Inoue R, and Tsukahara T. 2017. Dietary Probiotic Compound Improves Reproductive Performance of Porcine Epidemic Diarrhea Virus-Infected Sows Reared in a Japanese Commercial Swine Farm under Vaccine Control Condition. *Frontiers in Immunology* 8:1877. 10.3389/fimmu.2017.01877

Julia P, Phil H, and John B. 2007. Matching the grade correlation coefficient using a copula with maximum disorder. *Journal of Industrial & Management Optimization* 3:305-312. 10.3934/jimo.2007.3.305

Kashyap PC, Chia N, Nelson H, Segal E, and Elinav E. 2017. Microbiome at the Frontier of Personalized Medicine.

Mayo Clinic Proceedings 92:1855-1864. https://doi.org/10.1016/j.mayocp.2017.10.004

Kemp PF, and Aller JY. 2004. Bacterial diversity in aquatic and other environments: what 16S rDNA libraries can tell us. *FEMS Microbiology Ecology* 47:161-177. 10.1016/S0168-6496(03)00257-5

Kim J, Kim J, Kim Y, Oh S, Song M, Choe JH, Whang KY, Kim KH, and Oh S. 2018. Influences of quorum-quenching probiotic bacteria on the gut microbial community and immune function in weaning pigs. *Anim Sci J* 89:412-422. 10.1111/asj.12954

Langille MG, Zaneveld J, Caporaso JG, McDonald D, Knights D, Reyes JA, Clemente JC, Burkepile DE, Vega Thurber RL, Knight R, Beiko RG, and Huttenhower C. 2013. Predictive functional profiling of microbial communities using 16S rRNA marker gene sequences. *Nature Biotechnology* 31:814-821. 10.1038/nbt.2676

Liu ZX, Wei HK, Zhou YF, and Peng J. 2018. Multi-level mixed models for evaluating factors affecting the mortality and weaning weight of piglets in large-scale commercial farms in central China. *Anim Sci J*. 10.1111/asj.12963

Mao S, Zhang M, Liu J, and Zhu W. 2015. Characterising the bacterial microbiota across the gastrointestinal tracts of dairy cattle: membership and potential function. *Scientific Reports* 5:16116. 10.1038/srep16116

Mao S, Zhang R, Wang D, and Zhu W. 2012. The diversity of the fecal bacterial community and its relationship with the concentration of volatile fatty acids in the feces during subacute rumen acidosis in dairy cows. *BMC Veterinary Research* 8:237. 10.1186/1746-6148-8-237

Robinson MD, McCarthy DJ, and Smyth GK. 2010. edgeR: a Bioconductor package for differential expression analysis of digital gene expression data. *Bioinformatics* 26:139-140. 10.1093/bioinformatics/btp616

Schloss PD, Westcott SL, Ryabin T, Hall JR, Hartmann M, Hollister EB, Lesniewski RA, Oakley BB, Parks DH, Robinson CJ, Sahl JW, Stres B, Thallinger GG, Van Horn DJ, and Weber CF. 2009. Introducing mothur: open-source, platform-independent, community-supported software for describing and comparing microbial communities. *Applied and Environmental Microbiology* 75:7537-7541. 10.1128/AEM.01541-09

Schoster A, Arroyo LG, Staempfli HR, and Weese JS. 2013. Comparison of microbial populations in the small intestine, large intestine and feces of healthy horses using terminal restriction fragment length polymorphism. *BMC Research Notes* 6:91. 10.1186/1756-0500-6-91

Segata N, Izard J, Waldron L, Gevers D, Miropolsky L, Garrett WS, and Huttenhower C. 2011. Metagenomic biomarker discovery and explanation. *Genome Biology* 12:R60. 10.1186/gb-2011-12-6-r60

Shen TD. 2017. Diet and Gut Microbiota in Health and Disease. *Nestle Nutr Inst Workshop Ser* 88:117-126. 10.1159/000455220

Sommer F, and Backhed F. 2013. The gut microbiota-masters of host development and physiology. *Nature Reviews Microbiology* 11:227. 10.1038/nrmicro2974

Strube ML, Ravn HC, Ingerslev HC, Meyer AS, and Boye M. 2015. In situ prebiotics for weaning piglets: in vitro production and fermentation of potato galacto-rhamnogalacturonan. *Applied and Environmental Microbiology* 81:1668-1678. 10.1128/AEM.03582-14

Tian Y, Nichols RG, Cai J, Patterson AD, and Cantorna MT. 2017. Vitamin A deficiency in mice alters host and gut microbial metabolism leading to altered energy homeostasis. *J Nutr Biochem* 54:28-34. 10.1016/j.jnutbio.2017.10.011

Turnbaugh PJ, Ley RE, Mahowald MA, Magrini V, Mardis ER, and Gordon JI. 2006. An obesity-associated gut microbiome with increased capacity for energy harvest. *Nature* 444:1027-1031. 10.1038/nature05414

White JR, Nagarajan N, and Pop M. 2009. Statistical methods for detecting differentially abundant features in clinical

409 metagenomic samples. *PLoS Computational Biology* 5:e1000352. 10.1371/journal.pcbi.1000352

410

Table 1(on next page)

Tag number, length, and quality of the segmented samples in both the B25 and B70 groups

Sample	Chao1	ACE	Shannon	npShannon	Simpson	Coverage
B25_D1	13302.28742	23991.17495	4.38906	4.537154	0.049186	0.964905
B25_D2	14838.57089	28578.09001	5.133235	5.265367	0.023812	0.960314
B25_D3	13592.25623	22663.84525	4.394256	4.540638	0.049337	0.96531
B25_I1	14906.24286	33533.4322	5.071789	5.171834	0.056045	0.969094
B25_I2	13983.81579	29555.86254	5.117193	5.220857	0.04114	0.967932
B25_I3	12049.71166	27357.82181	4.286919	4.391756	0.123526	0.974135
B25_J1	9902.136364	15930.09663	3.49562	3.643879	0.168721	0.971338
B25_J2	23282.10606	43900.25354	5.760419	6.001067	0.021651	0.915859
B25_J3	8950.881696	14911.86895	3.316506	3.45679	0.152006	0.973494
B25_C1	17712.61468	35865.91558	5.782135	5.889584	0.011103	0.957613
B25_C2	10144.03175	20349.37991	4.208988	4.325446	0.041918	0.971516
B25_C3	13513.03778	28078.48698	4.636424	4.759541	0.041351	0.966969
B70_D1	8208.22	16204.03926	4.594705	4.675623	0.03065	0.978734
B70_D2	7691.035587	14503.70621	4.154997	4.235742	0.054827	0.981157
B70_D3	8609.120301	15425.4676	4.07753	4.180121	0.064076	0.977215
B70_I1	8417.993976	15752.73911	3.730674	3.839474	0.07122	0.976851
B70_I2	13385.71571	29314.05599	4.72353	4.836475	0.059948	0.969138
B70_I3	7175.217391	13093.34792	2.795669	2.895738	0.270206	0.982254
B70_J1	1823.466102	3097.659716	2.087158	2.124766	0.235761	0.994267
B70_J2	1965.478261	3337.176365	1.718008	1.76344	0.39248	0.99347
B70_J3	3434.638298	5322.936695	2.694431	2.748308	0.165643	0.990666
B70_C1	7172.0625	12711.82924	3.410237	3.50162	0.160898	0.982079
B70_C2	5604.911458	10149.60698	2.973876	3.052093	0.219155	0.985422
B70_C3	5431.927126	10738.78134	3.217852	3.298466	0.144869	0.984658

Table 2(on next page)

Alpha diversities of the segmented samples in both the B25 and B70 group

Sample ID	Total Tag Number	Total Tag length	Unique Tag Number	Unique Tag Total Length	Max Length	Min Length	N50	N90
B25_D1	88851	40487000	50995	23215392	479	301	462	441
B25_D2	85444	38891698	48899	22238506	479	301	461	441
B25_D3	91244	41414603	44901	20388941	479	301	466	441
B25_I1	85897	38546089	42127	18974409	468	314	441	440
B25_I2	65723	29931526	42988	19563017	478	318	461	441
B25_I3	83830	37792714	38639	17482746	472	313	441	440
B25_J1	78916	36039156	48931	22313808	478	301	461	441
B25_J2	74639	33814033	31772	14443701	478	326	460	441
B25_J3	83981	38419967	38428	17580118	479	307	461	441
B25_C1	90327	41540229	45558	20916181	479	303	461	444
B25_C2	82245	37489631	46900	21376857	479	321	461	441
B25_C3	90861	41775360	46685	21432798	479	303	461	444
B70_D1	83847	38229796	33670	15363351	479	397	461	441
B70_D2	88978	40500188	44888	20406438	479	301	461	441
B70_D3	87456	40245744	30644	14039932	479	308	467	441
B70_I1	84248	37999280	26891	12174039	469	364	441	441
B70_I2	82844	38104155	28173	12951148	469	318	466	441
B70_I3	82919	37600764	29899	13584709	477	434	461	441
B70_J1	90455	40638732	40690	18334381	476	303	441	440
B70_J2	83073	38111253	31639	14479164	478	301	466	443
B70_J3	84343	37923165	36685	16537239	470	339	441	440
B70_C1	85207	38768396	43736	19909095	479	308	461	441
B70_C2	89743	40293756	42202	18994317	469	382	442	441
B70_C3	91112	40971017	42557	19175549	472	307	442	441

1

Table 3(on next page)

Intragroup beta diversity matrices of the two groups

PeerJ Preprints | https://doi.org/10.7287/peerj.preprints.26893v1 | CC BY 4.0 Open Access | rec: 26 Apr 2018, publ: 26 Apr 2018

	B-25-D-	B-25-D-	B-25-D-	B-25-I-	B-25-I-	B-25-I-	B-25-J-	B-25-J-	B-25-J-	B-25-C-	B-25-C-	B-25-C-
B-25-D-		0.1505	0.1761	0.3691	0.2381	0.3061	0.1654	0.3234	0.2891	0.3006	0.2424	0.3192
B-25-D-	0.1505		0.1907	0.3768	0.2132	0.3224	0.1850	0.2991	0.2872	0.2809	0.2034	0.2914
B-25-D-	0.1761	0.1907		0.3682	0.2696	0.3398	0.2116	0.3393	0.3264	0.3143	0.2732	0.3228
B-25-I-1	0.3691	0.3768	0.3682		0.3313	0.2660	0.3303	0.3071	0.3290	0.3392	0.3783	0.3730
B-25-I-2	0.2381	0.2132	0.2696	0.3313		0.2913	0.2109	0.2640	0.2739	0.2259	0.1746	0.2466
B-25-I-3	0.3061	0.3224	0.3398	0.2660	0.2913		0.2881	0.3104	0.3042	0.3053	0.3392	0.3428
B-25-J-1	0.1654	0.1850	0.2116	0.3303	0.2109	0.2881		0.2972	0.2773	0.2554	0.2291	0.2737
B-25-J-2	0.3234	0.2991	0.3393	0.3071	0.2640	0.3104	0.2972		0.3090	0.2560	0.2821	0.2316
B-25-J-3	0.2891	0.2872	0.3264	0.3290	0.2739	0.3042	0.2773	0.3090		0.2837	0.2894	0.2959
B-25-C-	0.3006	0.2809	0.3143	0.3392	0.2259	0.3053	0.2554	0.2560	0.2837		0.2401	0.2004
B-25-C-	0.2424	0.2034	0.2732	0.3783	0.1746	0.3392	0.2291	0.2821	0.2894	0.2401		0.2480
B-25-C-	0.3192	0.2914	0.3228	0.3730	0.2466	0.3428	0.2737	0.2316	0.2959	0.2004	0.2480	

	B-70-D-	B-70-D-	B-70-D-	B-70-I-	B-70-I-	B-70-I-	B-70-J-	B-70-J-	B-70-J-	B-70-C-	B-70-C-	B-70-C-
B-70-D-		0.3333	0.3410	0.5787	0.5977	0.4402	0.3844	0.4911	0.3844	0.4323	0.4311	0.4231
B-70-D-	0.3333		0.2598	0.6676	0.6835	0.4052	0.2554	0.3900	0.3106	0.3039	0.3083	0.2897
B-70-D-	0.3410	0.2598		0.6651	0.6795	0.4541	0.2904	0.4162	0.3625	0.4114	0.3948	0.3901
B-70-I-1	0.5787	0.6676	0.6651		0.3004	0.4722	0.5809	0.5928	0.5152	0.6141	0.6022	0.5608
B-70-I-2	0.5977	0.6835	0.6795	0.3004		0.4676	0.5905	0.5787	0.5244	0.6336	0.6210	0.5746
B-70-I-3	0.4402	0.4052	0.4541	0.4722	0.4676		0.3703	0.3976	0.3444	0.3581	0.3548	0.3285
B-70-J-1	0.3844	0.2554	0.2904	0.5809	0.5905	0.3703		0.3430	0.2440	0.2751	0.2897	0.2782
B-70-J-2	0.4911	0.3900	0.4162	0.5928	0.5787	0.3976	0.3430		0.3560	0.3634	0.3458	0.3343
B-70-J-3	0.3844	0.3106	0.3625	0.5152	0.5244	0.3444	0.2440	0.3560		0.3160	0.3008	0.2702
B-70-C-	0.4323	0.3039	0.4114	0.6141	0.6336	0.3581	0.2751	0.3634	0.3160		0.2446	0.2374
B-70-C-	0.4311	0.3083	0.3948	0.6022	0.6210	0.3548	0.2897	0.3458	0.3008	0.2446		0.1660
B-70-C-	0.4231	0.2897	0.3901	0.5608	0.5746	0.3285	0.2782	0.3343	0.2702	0.2374	0.1660	

1. The beta diversities generated by comparing the small intestinal segments in the B70 group were significantly larger than those generated in the B25 group ($p < 0.01$). **2.** The beta diversities imputed by comparing cecum and each small intestinal segments were significantly higher in the B70 group ($p < 0.01$) than those in the B25 group.

Figure 1

Profile of the intestinal microbiota between 25 d and 70 d in Shanxi Black pigs

(A) Correlation coefficients of the segmented samples in both the B25 and B70 groups. **(B)** Multi-sample Shannon-Wiener curves of segmented samples in both the B25 and B70 groups. **(C)** Principal component analysis (PCA) plot of the segmented samples based on the OTU profiling.

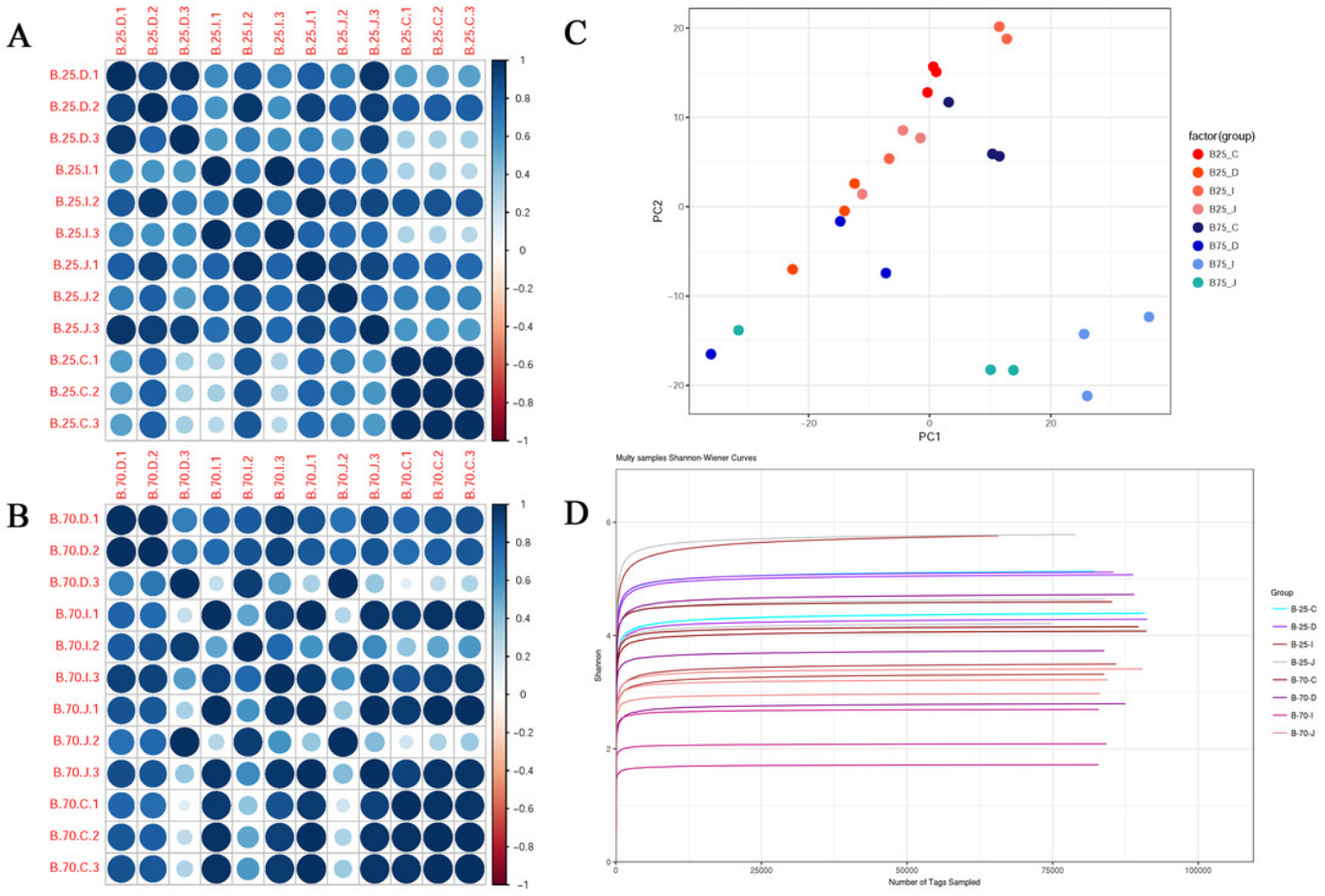

Figure 2

Relative abundances of sequences belonging to different phyla and genera

(A) Phylum distribution of the segmented samples in both the B25 and B70 groups. **(B)** Genera distribution of the segmented samples in both the B25 and B70 groups. **(C)** Shannon, ACE, Simpson, and Chao1 indices of the merged segments in both the B25 and B70 groups. (**1.** In both the B25 and B70 groups, the cecum segments exhibited significantly lower ($p < 0.01$) Simpson index values and higher ($p < 0.01$) Chao1, ACE and Shannon index values than in their respective SI segments; **2.** The SI in the B25 group had significantly higher Chao1, ACE and Shannon indices ($P<0.01$) and lower Simpson indices ($P<0.05$) than the SI in the B70 group. **3.** The cecum in the B25 group had significantly higher indices of Chao1 ($P<0.01$) and ACE ($P<0.05$) than the cecum in the B70 group.)

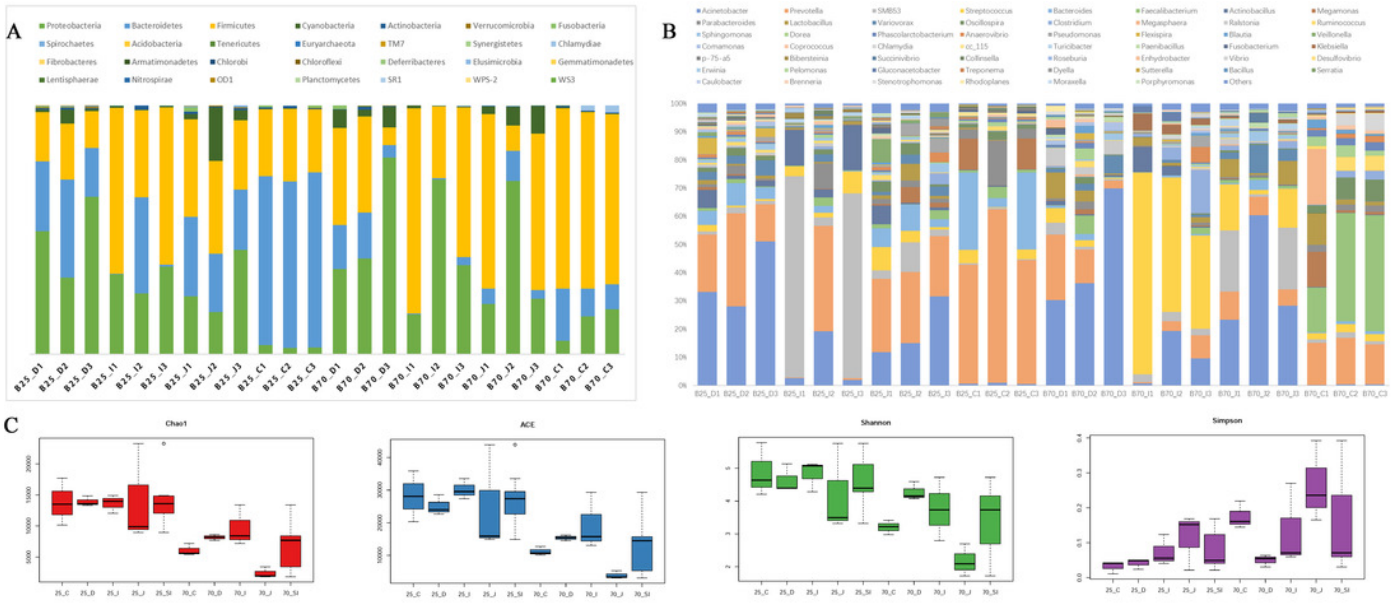

Figure 3

LEFse analysis revealed differentiated taxa

(A) Abundances of selected differentiated taxa in the B25 and B70 groups. **(B)** LDA scores of significantly differentiated taxa in the B25 and B70 groups. **(C)** Cladogram of differentiated taxa among the segments in the B25 and B70 groups.

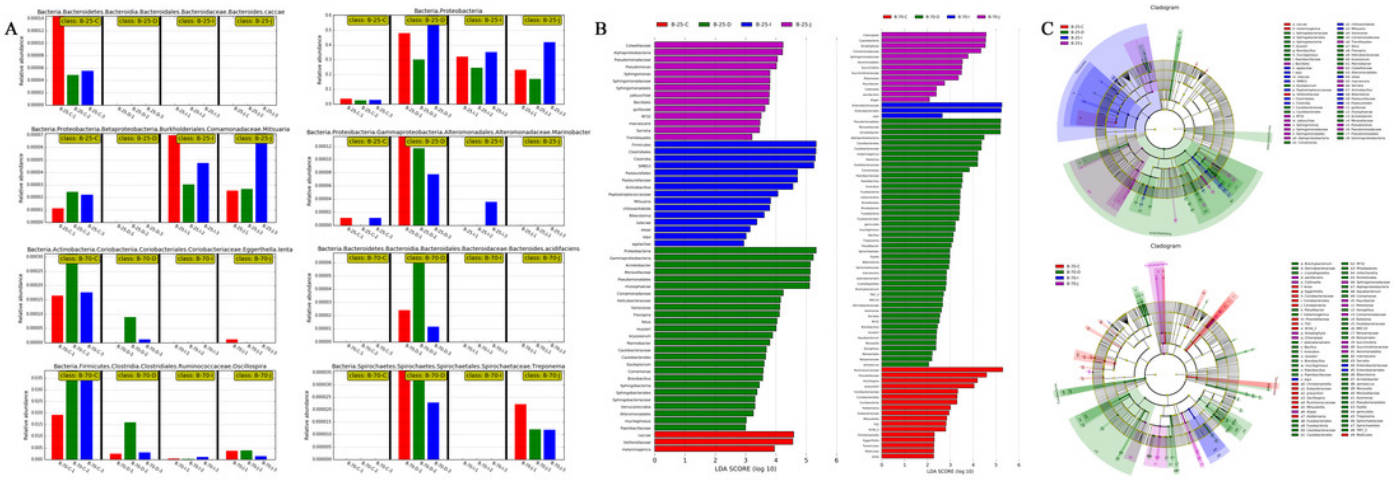

Figure 4

Intra group differentiated molecular functions

(A-C) Intra group differentiated molecular functions in the B25 group (A: segment correlation coefficients plot, B: significance and fold change volcano plot, and C: molecular function heatmap). **(D-F)** Intra group differentiated molecular functions in the B75 group (D: segment correlation coefficients plot, E: significance and fold change volcano plot, and F: molecular function heatmap.)

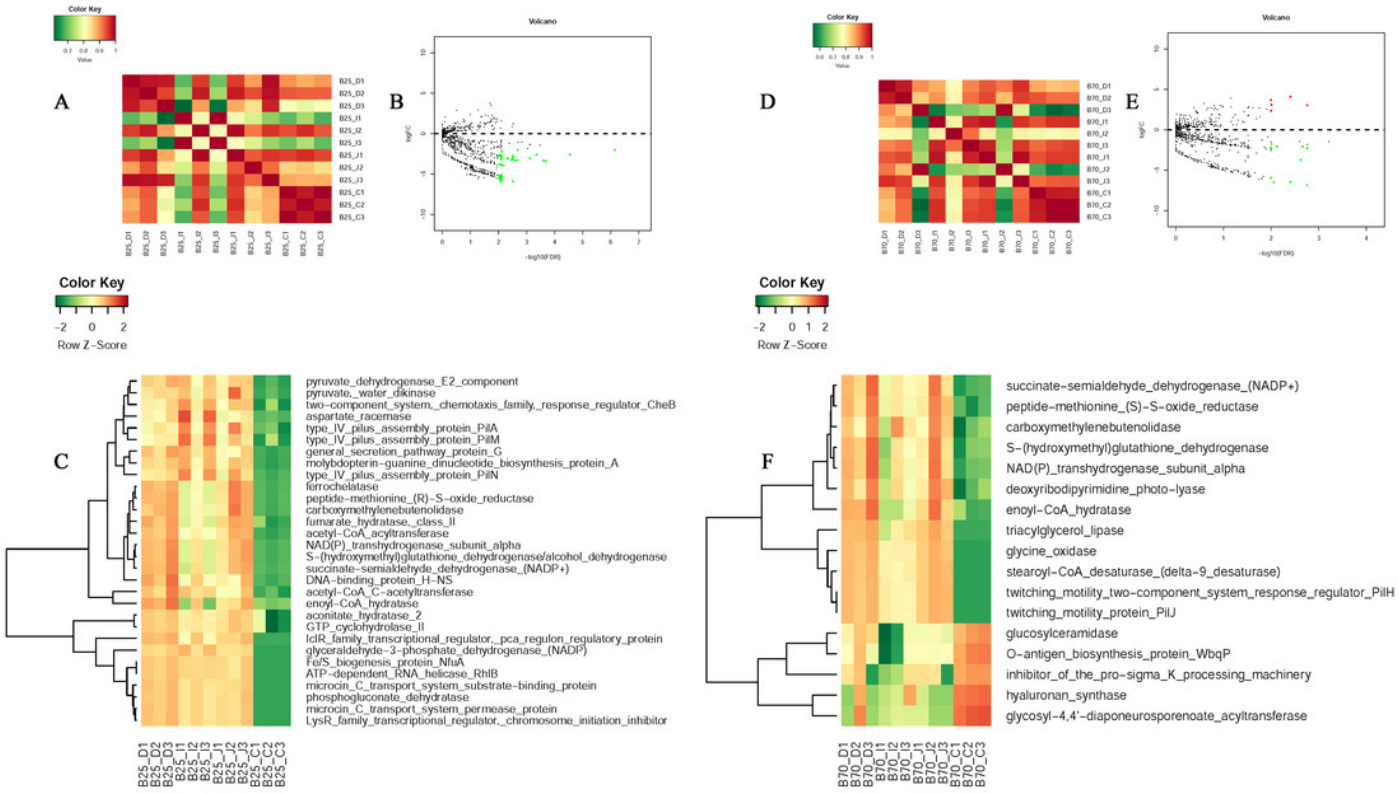

Figure 5

Inter group differentiated molecular functions and pathways

(A) Differentiated molecular functions heatmap of the I segments between the B25 and B70 groups. **(B)** Differentiated molecular functions heatmap of the C segments between the B25 and B70 groups. **(C-F)** Differentiated pathway enrichment based on differentiated taxa in D, J, I, and C segments between the B25 and B70 groups, as revealed by Metastat, respectively.